International Journal of Pharmaceutics 401 (2010) 16–24

Contents lists available at ScienceDirect

International Journal of Pharmaceutics

journal homepage: www.elsevier.com/locate/ijpharm

Ultrasound-enhanced intrascleral delivery of protein

Alex Chi Yeung Cheung[a], Yu Yu[b], David Tay[c], Hoi Sang Wong[a], Rutledge Ellis-Behnke[c], Ying Chau[a,b,*]

[a] Department of Chemical and Biomolecular Engineering, The Hong Kong University of Science and Technology, Hong Kong, China
[b] Bioengineering Program, The Hong Kong University of Science and Technology, Hong Kong, China
[c] Department of Anatomy, Li Ka Shing Faculty of Medicine, The University of Hong Kong, Hong Kong, China

ARTICLE INFO

Article history:
Received 28 May 2010
Received in revised form 30 July 2010
Accepted 1 September 2010
Available online 22 September 2010

Keywords:
Ocular delivery
Non-invasive
Posterior segment
Sonophoresis
Cavitation

ABSTRACT

We aim to investigate ultrasound on enhancing protein penetration into the sclera, a non-invasive method to overcome the first barrier in taking the transscleral route for delivering therapeutics. Rabbit eyes were immersed in a fluorescein isothiocyanate conjugated bovine serum albumin solution. The distances of protein penetration, with and without ultrasound (30 s continuous wave, 1 MHz, 0.05 W/cm^2) applied on the sclera, and at different immersion time intervals (0, 5, 15, 30 and 60 min), were measured by examining the cryo-sectioned tissues under fluorescence microscope (≥60 measurements from 3 eyes for each condition). Retina was examined for structural damage by histology. It was found that ultrasound enhances the intrascleral penetration of protein, increasing the diffusivity by 1.6-folds while causing no damage to the retinal tissues. This physical modulation of the sclera is temporary, as evident by the restoration of the diffusional resistance at 15 min after ultrasound treatment. The negligible effect of ultrasound-induced convection and the minimal temperature rise (<0.5 °C), together with cavitation detected by acoustic emission and a decreased penetration distance at higher ultrasound frequency (30 s continuous wave, 3 MHz, 0.05 W/cm^2), suggest that cavitation is a possible mechanism for increasing the permeability of the sclera for diffusive transport.

© 2010 Elsevier B.V. All rights reserved.

1. Introduction

Therapeutic molecules for treating diseases at the posterior segment of the eye are emerging. Among them, protein drugs represent an important class. Examples include Lucentis® (ranibizumab) that suppresses choroidal neovascularization in age-related macular degeneration (AMD) (Kourlas and Abrams, 2007; Zarbin and Szirth, 2007) and growth factors such as ciliary neurotrophic factor (CNTF) that halt or reverse neural degeneration in the retina (Sieving et al., 2006). However, an effective and non-invasive method for delivering macromolecular drugs to the eye is lacking.

Topical administration of eye drops is the easiest way to deliver drugs. However, only less than 1/10^8 of protein drug may reach the back of the eye (Nomoto et al., 2009). Systemic delivery is another way to deliver drugs to the posterior segment, but a large amount of drugs are needed to reach the therapeutic level since the blood-retinal barrier (BRB) restricts the influx of drugs to the retina. Furthermore, undesirable distribution to other parts of the body may result in side effects (Geroski and Edelhauser, 2001). For emerging therapeutics that include proteins and nucleic acids, systemic delivery also suffers from the problem of drug lability, in such a way that biomolecules may be degraded before they reach the eye. The most direct and effective practice is intravitreal injection. However, this invasive approach carries the risk of cataract, retinal detachment, vitreous hemorrhage and endophthalmitis, especially when multiple injections are needed as in the case of chronic eye diseases (Janoria et al., 2007).

Transscleral route has attracted much interest as a potential path for delivering therapeutics into the posterior segment. There are several advantages: firstly, diffusion of macromolecules through the sclera is feasible, as demonstrated in the *ex vivo* diffusion experiments using rabbit sclera by Ambati et al. (2000). Secondly, the distance for drug molecules to penetrate into the posterior segment is shorter via the transscleral than the transcorneal route. After diffusing through the sclera, drug molecules are closer to the vicinity where most posterior diseases occur: the choroid and the retina.

A less invasive method has been developed by Jiang et al. using microneedles to deliver soluble molecules, nanoparticles and microparticles intrasclerally (Jiang et al., 2009). Using this approach, controlled drug release within the sclera was made possible by delivering drug-encapsulated nanoparticles and microparticles into the deeper sclera. Drug molecules could then diffuse to the neighboring posterior ocular tissues. Another tech-

* Corresponding author at: The Hong Kong University of Science and Technology, Department of Chemical and Biomolecular Engineering, Clear Water Bay, Kowloon, Hong Kong, China. Tel.: +852 2358 8935; fax: +852 2358 0054.
E-mail address: ying.chau@ust.hk (Y. Chau).

0378-5173/$ – see front matter © 2010 Elsevier B.V. All rights reserved.
doi:10.1016/j.ijpharm.2010.09.001

nique, transscleral iontophoresis, has been employed by a number of research groups to deliver drugs to the posterior segment using electric field. However, iontophoresis may be limited to charged drugs (Myles et al., 2005). Patients also complained about the burning sensation (Parkinson et al., 2003).

Here, we explore the use of ultrasound to deliver protein non-invasively into the sclera in order to take advantage of the transscleral route. Ultrasound has been used extensively for diagnostic, therapeutic and surgical purposes both within and outside ocular areas (Kremer et al., 1985; Pavlin et al., 1991; McDermott et al., 1997). We are inspired by the application of ultrasound in transdermal drug delivery. It was found that ultrasound could disrupt the outermost layer of the skin temporarily and increase the permeability of the skin. Mitragotri et al. delivered insulin and other protein molecules across the animal and human skin using this approach (Mitragotri et al., 1995). However, limited research has been performed to use ultrasound in ocular drug delivery. It was reported that low-frequency ultrasound applied to the corneal surface increased the amount of sodium fluorescein delivered to the aqueous humor by 10 times (Zderic et al., 2002, 2004a,b). However, no one has investigated the effects of ultrasound in delivering macromolecules through the sclera. In this report, we perform *ex vivo* experiments using rabbit eyes and track albumin penetration using a fluorescence microscope following a short ultrasound exposure. We aim to measure the ultrasound enhancement of protein transport, propose a potential mechanism, and provide an initial assessment of the feasibility of this method.

2. Materials and methods

2.1. Materials

FITC–BSA of molecular weight 65 kDa was obtained from Sigma (St. Louis, MO, USA). An aqueous solution containing 0.1% FITC–BSA (Ambati et al., 2000) was prepared by dissolving FITC–BSA in a modified Ringer's solution having the following composition: 122 mM of sodium chloride, 5.1 mM of potassium chloride, 3 mM of disodium phosphate, 25 mM of sodium bicarbonate, 1 mM of calcium chloride dihydrate, 1 mM of magnesium chloride hexahydrate, 5.1 mM of dextrose, and 0.6 mM of glutathione disulfide. This solution is adjusted to pH 7.4 and is denoted as "saline buffer" hereinafter. All chemicals were of analytical grade and purchased from Sigma (St. Louis, MO, USA). All samples were light-protected until the fluorescence measurement.

2.2. Ultrasound device and its calibration

The ultrasound device (BTL-4000, BTL Industries Inc., Clark, NJ, USA) contains a focused transducer with a probe size of 1 cm^2. The device is designed for physiotherapeutic use. Both 1 and 3 MHz ultrasound of continuous wave are generated by the same transducer. The driving frequency (which is the same as the pulse repetition frequency of a continuous wave) was measured by a membrane hydrophone (HMB-0500, Onda Corp., Sunnyvale, CA, USA) connected to an oscilloscope (Tektronix, Beaverton, OR, USA). The center frequency was confirmed to be 1 and 3 MHz, respectively. The peak negative pressure was detected with the same set-up for calculating the mechanical index (Supplementary information). The ultrasound intensity was calibrated by the calorimetric method (Zderic et al., 2002). Briefly, 15 ml of water was put into a plastic test tube with cotton wrap around as an insulating layer and was sonicated by the ultrasound device for 5 min. The temperature rise was measured by a thermocouple (206-3738, RS Components Ltd., Hong Kong). The ultrasound intensity was calculated by the following equation:

$$I = \frac{m_{\text{water}} C_{p,\text{water}}}{A} \frac{\Delta T}{\Delta t}$$

where I is the average intensity [W/cm^2], m_{water} is the mass of water [g], $C_{p,\text{water}}$ is the specific heat capacity of water, ΔT is the change in temperature, A is the cross-sectional area of the transducer probe (1 cm^2), and Δt is the time for the calorimetric test.

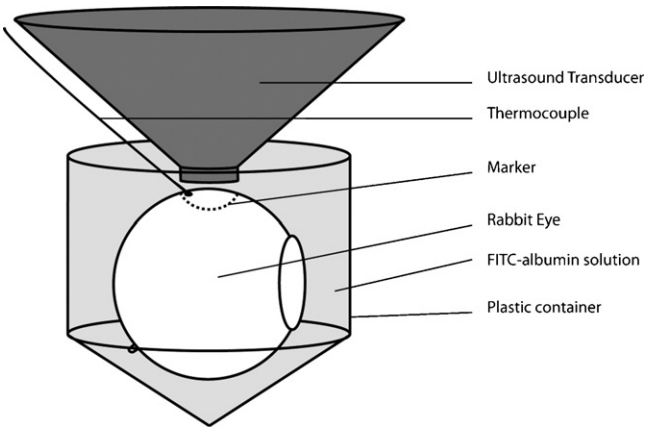

Fig. 1. The setup of *ex vivo* ultrasound experiments. The eye from a New Zealand White Rabbit is immersed in 4 ml of 0.1% FITC–albumin in saline buffer. The region of ultrasound application is labeled with a marker. The ultrasound probe is placed directly above the sclera near the equator and was in contact with the FITC–albumin solution. The scleral surface temperature before and after ultrasound application is measured by a thermocouple.

2.3. Ex vivo experiments

2.3.1. Animals and experimental set-up

The use of animals was approved by the local animal ethics committee. The eyes of New Zealand White Rabbits (aged 6–9 months) were enucleated immediately after the rabbits were sacrificed. At least 3 eyes from different rabbits were used for each experimental or control condition. The eyes were kept on ice for transporting from the animal facility to the laboratory and this time lag never exceeded 2 h to ensure tissue freshness. Before an experiment began, the eye was washed with saline buffer at room temperature to remove the blood on the eye surface, and all the periocular tissues (conjunctiva, muscles and orbital fat) were removed. The optic nerve was sealed with Vaseline®, which was insoluble in saline buffer and stayed in place after application. This preparation step normally took 10–15 min and by then the eye was equilibrated to room temperature. Saline buffer was used to keep the eye hydrated during the preparation. The experimental set-up is schematically shown in Fig. 1. The eye was immersed in a container filled with 4 ml of 0.1% FITC–BSA solution or saline buffer. The ultrasound transducer probe of 1 cm^2 was positioned approximately 1–3 mm above the sclera near the equator. The zone of ultrasound application was labeled with a marker. Ultrasound at either 1 or 3 MHz with an intensity of 0.05 W/cm^2 was applied for 30 s. The eye was either immersed in 0.1% FITC–BSA, a non-fluorescent 0.1% BSA solution, or saline buffer during the ultrasound application and immersion continued for different lengths of time. (Details of specific experiments are found in the subsequent subsections.) To avoid fluorescence bleaching, the set-up was covered with aluminum foil so that the FITC–BSA solution was kept in a dark environment. Experiments were conducted at room temperature ($20 \pm 2\,^{\circ}C$), which was regulated by the laboratory's air-conditioning system. The scleral surface temperature at the ultrasound application zone before and after treatment was measured using a thermocouple (206-3738, RS

Components Ltd., Hong Kong). Controls were done by immersing the eye for the corresponding time intervals without ultrasound application.

2.3.2. Evaluation of the enhancement by ultrasound on protein penetration

The general procedure was described in Section 2.3.1. Ultrasound of 1 MHz was used in this series of experiments. The eye was placed in FITC–BSA solution when ultrasound was applied for 30 s. Immersion in the protein solution continued for another 5, 15, 30 and 60 min. For control, no ultrasound was applied.

2.3.3. Examination of the duration of ultrasound enhancement

The general procedure was described in Section 2.3.1. Here, we aim to verify the hypothesis that the ultrasound-enhanced protein penetration is temporary and that the effect will disappear in 15 min. The eye was placed in the (colorless) saline solution when ultrasound of 1 MHz was applied for 30 s. Immersion continued in the saline solution for 15 min. Then the eye was transferred to FITC–BSA solution and was immersed for another 15 min. The result from this experiment was compared with that of which the eye was not ultrasound-treated and immersed in FITC–BSA for 15 min.

2.3.4. Evaluation of the repeatability of ultrasound enhancement

The general procedure was described in Section 2.3.1. The eye was placed in a non-fluorescent BSA solution when ultrasound of 1 MHz was applied for 30 s. Immersion continued for 15 min. After this lapse, the eye was transferred to FITC–BSA solution and ultrasound of the same condition was applied again. Immersion in the fluorescent protein solution continued for another 15 min. The result of this experiment was compared with that of which the eye was ultrasound-treated once and was immersed in FITC–BSA for 15 min.

2.3.5. Evaluation of the role of bulk flow due to acoustic streaming

The general procedure was described in Section 2.3.1. The eye was placed in FITC–BSA solution when ultrasound of 1 MHz was applied for 30 s. The eye was immediately removed from the protein solution and frozen after ultrasound treatment.

2.3.6. Evaluation of the effect of changing ultrasound frequency

The general procedure was described in Section 2.3.1. The eye was placed in FITC–BSA solution when ultrasound of 3 MHz was applied. The immersion in the protein solution continued for another 15 min. The results was compared with that of which ultrasound of 1 MHz was applied under otherwise the same conditions.

2.4. Measurement of protein penetration

2.4.1. Cryo-sectioning

Immediately after the *ex vivo* experiment, the whole eye was washed by optimum cutting temperature medium (O.C.T) (Leica, Wetzlar, Germany) and immersed in a mould filled with O.C.T, followed by quick-freezing in liquid nitrogen. 10 μm thick sections across the marked ultrasound application zone of the eye were cut using a cryostat (CM1850, Leica, Wetzlar, Germany). The eye was sectioned parallel to the equator and perpendicular to the sagittal plane. Thus for each sectioned slide, both the marked zone and the unmarked zone are present and examined. Polylysine-coated slides (Bio-High Technology, Hebei, China) were used for collecting the tissue sections.

2.4.2. Analysis of fluorescence images

All images were acquired using a fluorescence microscope (BX 41, Olympus, Center Valley, PA, USA). The image of the sclera was captured under optical mode, and FITC–BSA penetration into the sclera was captured under the fluorescence mode (bandpass filter: 460–490 nm, dichroic mirror: 505 nm, barrier filter: 515 nm, exposure time: 1000 ms). The pictures shown in the report were merged images of these two modes, allowing the simultaneous visualization of the ocular structures and the protein penetration. The thickness of the sclera and the penetration distance of FITC–BSA were obtained using the software SPOT® (version 4.6, Diagnostic Instruments, Inc., MI, USA). Penetration distance was measured based on the green color of the fluorescence image. We have used the same microscope setting and exposure time in capturing images from different experiments in order to obtain comparable contrast in the fluorescence images. The black background was used to define the baseline at where green-colored FITC–BSA has not penetrated. The distance from the sclera surface to the deepest depth at which the green color intensity is just above the baseline represents the penetration distance.

For each experiment or control, at least 3 eyes from different rabbits were used and at least 15 sections were obtained for each eye. From these sections, at least 20 measurements were obtained for each eye. Unless damage or artifact was made to the sclera during cryo-sectioning (e.g. tearing or flipping) that would prevent the accurate measurement of the penetration distance, sections were kept for measurement and there were no less than 3 qualified sections for each eye. In each section, random measurements were made in all regions, including the left, right, top center and bottom center.

2.5. Calculation of intrascleral diffusivity

The one-dimensional diffusion model describing the penetration distance (L), diffusivity (D) and time of diffusion (t) is given by the equation below (Saltzman, 2001):

$$L = \sqrt{2Dt} \tag{1}$$

A plot of the penetration distance versus the square root of time yields a straight line. The diffusivity is calculated from the slope, which equals $\sqrt{2D}$.

The diffusivity measured at room temperature is converted to the value at 37 °C according to Stokes–Einstein equation, which gives:

$$\frac{D_{37}}{D_{20}} = \frac{310\,\mathrm{K} \times \eta_{20}}{293\,\mathrm{K} \times \eta_{37}} \tag{2}$$

where D and η are diffusivity and viscosity, respectively, with the temperature designated at the subscript. Since our experiment was conducted in dilute buffer solution, the viscosity of water is used.

2.6. Detection of cavitation by acoustic emission

The method of detection was according to Farny et al. (2009). Briefly, The 1 cm^2 probe of the ultrasound device (Section 2.2) was connected with a cylindrical tube of 14 mm diameter and 15 mm height made with silicone rubber. The tube was filled with water, and a single-element ultrasonic atomizing transducer of 1.70 MHz central frequency (S-UAT03A, Sound Components Limited, Hong Kong) was placed at the other end of the tube. The 1 cm^2 ultrasound probe acted as the transmitter and the single-element transducer as the receiver. The ultrasound device was set to produce a 1 MHz ultrasound continuous wave at 0.05 W/cm^2 (Section 2.2), and the receiver was connected to an oscilloscope (TDS1002B, Tektronix, Beaverton, OR, USA). The signal generated by the receiver in response to the ultrasound produced by the transmitter was recorded by the oscilloscope. The oscilloscope was set to Fast-Fourier-Transform (FFT) mode to display the frequency spectrum.

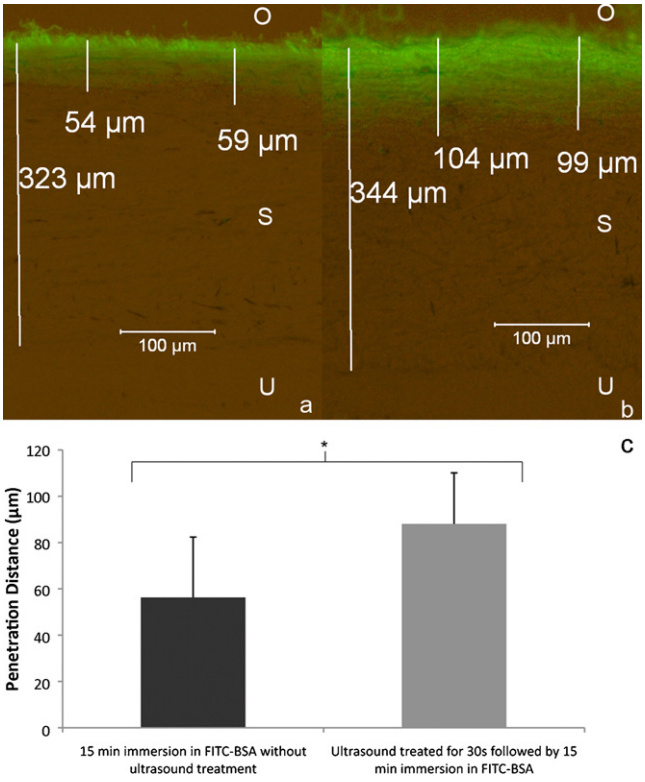

Fig. 2. The effect of ultrasound on the intrascleral penetration of FITC–BSA. Representative cryo-sections illustrate the protein penetration into the rabbit sclera: (a) harvested from the control eye with no ultrasound treatment; (b) harvested from the eye that was exposed to 30 s of ultrasound at 1 MHz and 0.5 W/cm^2. In both, eyes were immersed in the protein solution for 15 min. The green color is from the fluorescent tag of the protein. S: sclera; O: orbital side; U: uveal side. The mean and standard deviation are shown in (c), averaging from over 80 measurements and 4 eyes for each condition (*$p < 0.05$). (For interpretation of the references to color in this figure legend, the reader is referred to the web version of the article.)

2.7. Histological study

The eye was immersed in saline buffer and ultrasound was applied as described above. To preserve the ocular tissues, 100 μl of 4% paraformaldehyde was injected into the eye via the optic nerve and the eye was then immersed in 4% paraformaldehyde for 1 day. After fixation, the eye was halved by a sharp razor on ice with sodium chloride added. The eyecup obtained (that is, the eye with the anterior chamber removed) was then cryoprotected by immersing in 30% sucrose overnight. After cryoprotection, O.C.T was added to displace the viterous inside the eyecup. The eyecup was embedded in O.C.T and was frozen in liquid nitrogen for sectioning. H&E stain was used to visualize the tissues.

2.8. Statistical analysis

Data (shown in Figs. 2–4 and 6) were analyzed using unpaired Student's *t*-test. The difference was considered statistically significant when *p*-value fell below 0.05.

3. Results

3.1. Enhancement of protein penetration by ultrasound into the sclera

The purpose of this study is to investigate the effects of ultrasound on intrascleral protein transport. The penetration distance of FITC–BSA was measured after cryo-sectioning the ocular tissues. Fig. 2 compares the results with and without ultrasound after the eyes were immersed in the protein solution for 15 min. Representative cryo-sections are shown. In the absence of ultrasound, FITC–BSA penetrated to 56.3 ± 26.1 μm by passive diffusion, which was 19 ± 9% of the thickness of the sclera. (The full thickness of the rabbit sclera was found to be 301.7 ± 26.1 μm from averaging the measurements of 56 sclera sections.) A brief application (30 s) of low-power ultrasound increased the penetration distance to 88.0 ± 22.0 μm, which was 29 ± 7% of the thickness of the sclera. The difference in the intrascleral penetration was statistically significant ($p < 0.05$).

3.2. Duration and repeatability of ultrasound-enhanced penetration

There appeared to be a short time window in which the sclera permeability for protein was improved by ultrasound. In this experiment, the ultrasound-treated eye was first immersed in the colorless saline buffer for 15 min before placing it in the FITC–BSA solution. If the effect of ultrasound halts after 15 min, the protein penetration distance is expected to resemble the control without ultrasound. Indeed, no significant difference was observed between the control eye and the ultrasound-treated eye, when there is a 15 min time lapse between ultrasound treatment and protein introduction ($p = 0.34$, Fig. 3).

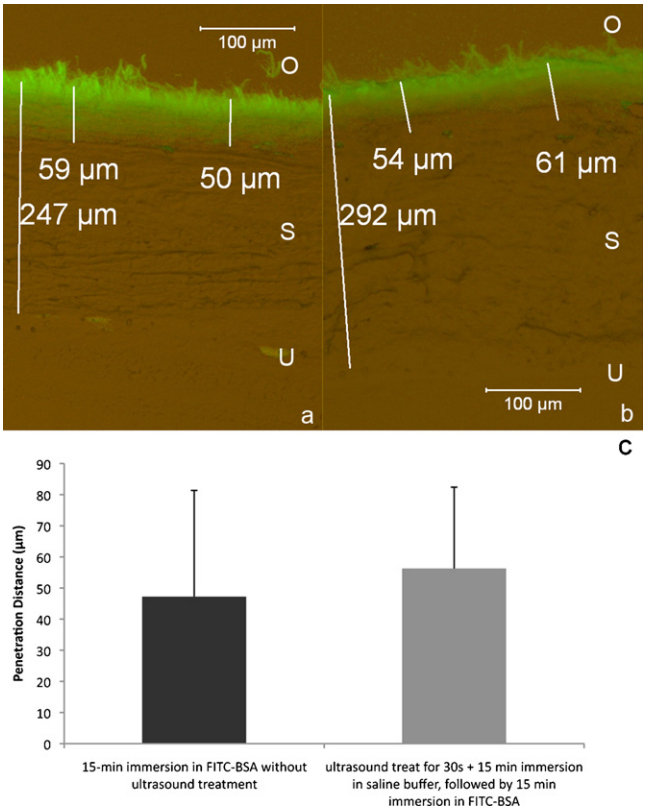

Fig. 3. The effect of time lapse on ultrasound enhancement. Representative cryo-sections show the penetration of fluorescent green colored FITC–BSA into the rabbit sclera when: (a) the eye was immersed in FITC–BSA solution without prior ultrasound treatment (control); (b) the eye was treated in ultrasound while in saline buffer, remained immersed in the colorless buffer for 15 min and then transferred to FITC–BSA solution for another 15 min. S: sclera; O: orbital side; U: uveal side. The mean and standard deviation are shown in (c), averaging from over 60 measurements and 3 eyes for each condition. No statistical significance was found between the two groups ($p = 0.34$). (For interpretation of the references to color in this figure legend, the reader is referred to the web version of the article.)

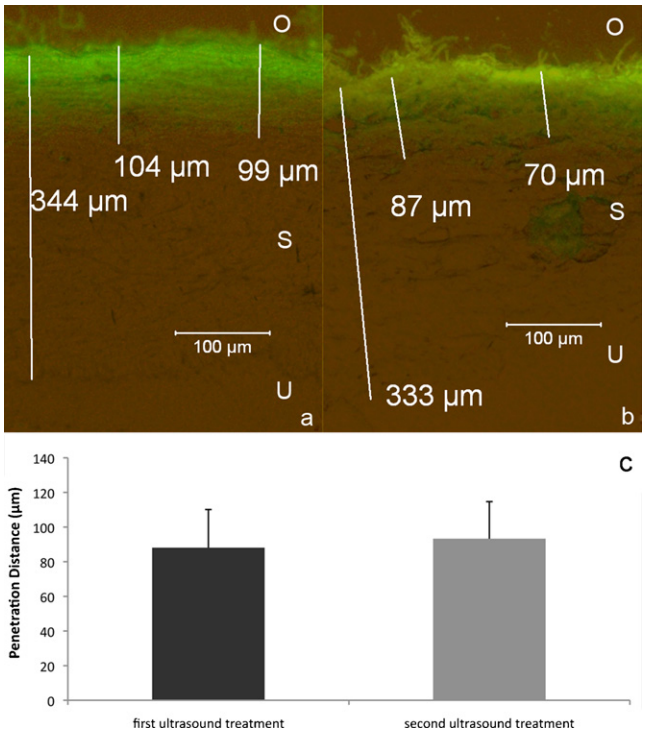

Fig. 4. Reproducibility of ultrasound-enhanced protein transport. Representative cryo-sections show the extent of FITC–BSA penetration into the rabbit sclera: (a) at 15 min after one ultrasound treatment; (b) at 15 min after the second ultrasound treatment. Here, ultrasound was first applied to the eye immersed in a non-fluorescent protein solution, after which the eye was transferred to FITC–BSA solution for the second ultrasound treatment. S: sclera; O: orbital side; U: uveal side. The mean and standard deviation are shown in (c), averaging from over 80 measurements and 4 eyes for each condition. No statistical significance was found between the two groups ($p = 0.37$).

In addition to being temporary, the enhancement by ultrasound was repeatable. Fig. 4b shows the penetration distance of FITC–BSA when ultrasound was applied first in a non-fluorescent protein solution, lapsed for 15 min, after which the eye was transferred to FITC–BSA solution and ultrasound was applied again. The intrascleral penetration distance was comparable to the case in which ultrasound was applied only once to the eye submerged in FITC–BSA ($p = 0.21$, Fig. 4).

3.3. Mechanism for the improvement of protein transport

Experiments were performed to shed light on the mechanism underlying the ultrasound-enhanced intrascleral protein transport. The contribution of thermal effects was gauged by the increase in temperature on the scleral surface. The rise was less than 0.5 °C under the current operating conditions. According to the estimation by Stokes–Einstein equation (Edward, 1970), the increase in diffusivity from this temperature rise alone is less than 0.2% (Supplementary information).

The role of acoustic streaming was assessed by measuring the protein penetration during the application of ultrasound (as opposed to after the ultrasound). This allowed us to observe if ultrasound-induced unidirectional bulk flow (Clarke et al., 2004; Lavon and Kost, 2004) carries protein deep into the sclera. To minimize the time for diffusion, the eye was frozen immediately after the ultrasound treatment. FITC–BSA was found to stay near the scleral surface (Fig. 5), with a negligible penetration depth of 15.8 ± 5.7 μm. This was in contrast to the much deeper penetration that occurred when time was given for diffusion after the ultrasound application (Fig. 2b).

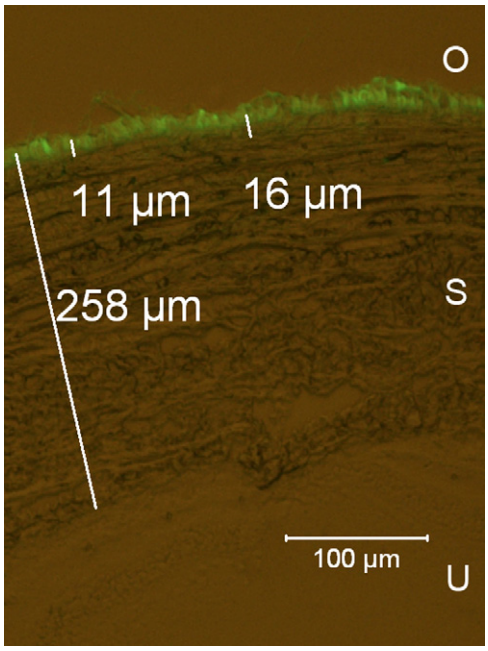

Fig. 5. Intrascleral protein penetration in the absence of diffusion time after ultrasound application. A representative cryo-section taken from a data set of over 60 measurements and 3 eyes is shown. S: sclera; O:orbital side; U: uveal side.

We varied the frequency of ultrasound to discern the likelihood of the contribution of cavitation and ultrasound-induced mechanical stress on the sclera (Fig. 6). While the effect of cavitation decreases with the ultrasound frequency (Lavon and Kost, 2004), the effect of mechanical stress increases with frequency (Van Krevelen, 1976). We found that the intrascleral penetration distance dropped from 88.0 ± 22.0 to 56.8 ± 10.7 μm when we elevated the frequency from 1 to 3 MHz ($p < 0.05$). The presence of bubble activity due to ultrasound-induced cavitation was detected by the measurement of acoustic emission. Peaks at harmonic frequencies (2 and 3 MHz) on the frequency spectrum indicate the stable oscillations of bubbles (Fig. 7a). The absence of peaks at subharmonic frequencies (0.5 and 0.25 MHz) indicate that the level of transient cavitation is negligible (Fig. 7b) (Leighton, 1994a, 1995).

3.4. Increase in intrascleral diffusivity of protein

When the penetration distance was plotted against the square root of time, linear graphs were obtained, supporting that diffusion

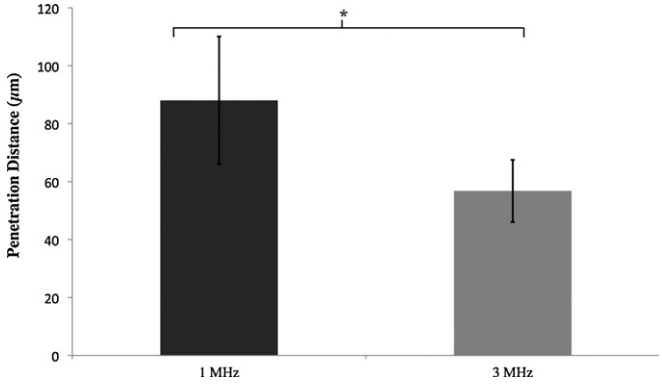

Fig. 6. The effect of ultrasound frequency on intrascleral protein penetration. The penetration distances of FITC–BSA at 15 min after an ultrasound application of 30 s at 1 and 3 MHz at 0.5 W/cm^2 are shown. The mean and standard deviation are calculated from over 80 measurements and 4 eyes for each condition (*$p < 0.05$).

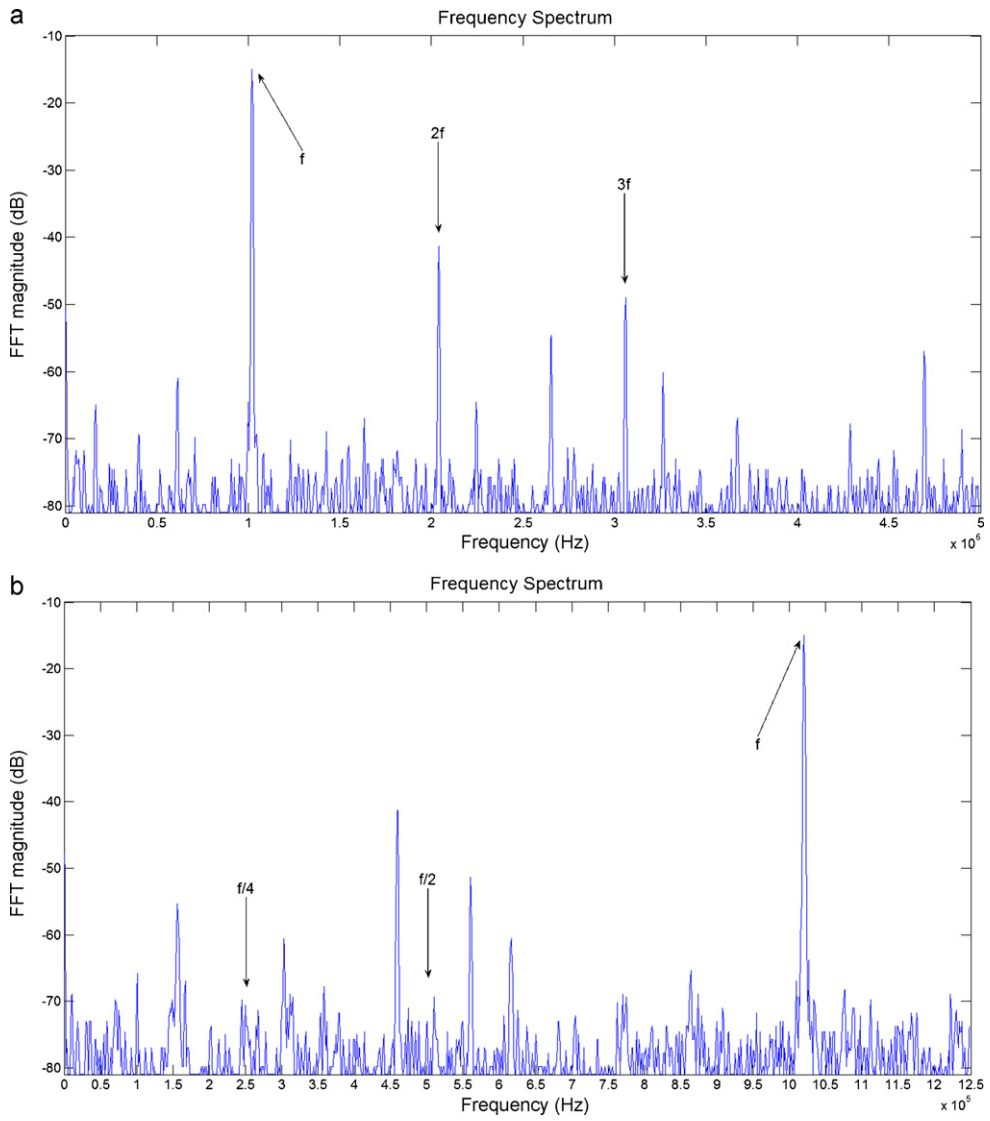

Fig. 7. Frequency spectrums for ultrasound wave at 1 MHz (f) and 0.05 W/cm^2. Peaks at harmonic frequencies (2f and 3f) are present in the spectrum showing the range 0–5 MHz (a). Peaks at subharmonic frequencies (f/2 and f/4) are absent in the spectrum showing the range 0–1.2 MHz (b).

was the dominated mode of transport (Fig. 8) (Saltzman, 2001). Intrascleral diffusivity at 37 °C was calculated from the slopes of the graphs. In the first 15 min, the diffusivity of FITC–BSA was increased by 1.6 times as a result of ultrasound treatment, from $(3.90 \pm 0.13) \times 10^{-8}$ to $(6.17 \pm 0.20) \times 10^{-8}$ cm^2/s. The slope measuring the protein diffusivity was flattened after 15 min. Using the data from 15 to 60 min post-ultrasound, the intrascleral diffusivity of FITC–BSA was calculated to be $(3.66 \pm 0.21) \times 10^{-8}$ cm^2/s. The difference between this value and the diffusivity without ultrasound treatment is statistically insignificant.

3.5. Examination of retinal integrity after ultrasound treatment

The temperature rise on the sclera was less than 0.5 °C and the mechanical index of the current setting was estimated to be 0.0493 (Supplementary information). Both parameters comply with the FDA guideline for the use of ultrasound in ophthalmic applications. To assess if ultrasound application causes any structural damage to the retina, cryostat sections of the ultrasound-treated eye were stained with H&E and examined under a microscope (Fig. 9). No apparent change to the cytoarchitecture of the retina or other ocular structures (including the sclera, choroid, Bruch's membrane)

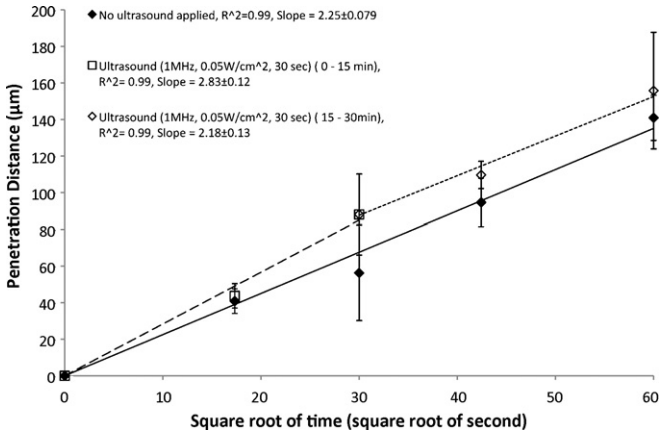

Fig. 8. Calculation of intrascleral diffusivity of FITC–BSA. The values were deduced from the slopes in the graphs plotting penetration distance against the square root of time. Linear regression is shown as dotted line for ultrasound treatment and as solid line for control (without ultrasound application), respectively. The diffusivity at 37 °C with ultrasound treatment was found to be 6.17×10^{-8} cm^2/s in the first 15 min and 4.18×10^{-8} cm^2/s from 15 to 60 min. The diffusivity in the control was 3.90×10^{-8} cm^2/s.

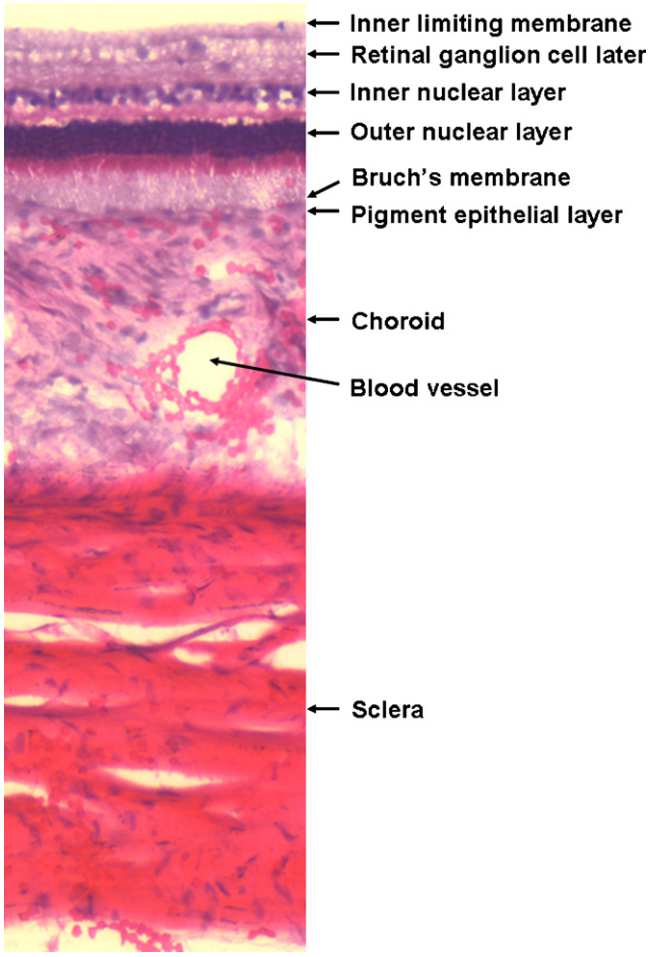

Fig. 9. Histological assessment of the effect of ultrasound on ocular structures. Tissue sections were prepared with hematoxylin and eosin (H&E) stain from a rabbit eye exposed to 30 s of ultrasound at 1 MHz and 0.5 W/cm^2. Objective = 10×.

was observed (For histological examination of ocular structures in a normal rabbit, readers are referred to Prince and McConnell, 1964.) The ultrasound treatment did not seem to cause retina detachment or deformation of the retinal layer at the area of the treated zone.

4. Discussion

Sclera is an attractive portal for delivering macromolecular therapeutic molecules to the back of the eye since high molecular weight compounds, including dextrans, polyethylene glycols and globular proteins (Hamalainen et al., 1997; Edwards and Prausnitz, 1998; Ambati et al., 2000) are found to be permeable to this outermost barrier in the posterior segment. However, the periocular clearance and the outward bulk fluid flow arising from osmotic or hydrostatic pressure decrease the amount of drugs that can be effectively delivered. The choroid-Bruch's membrane and retina pigmented epithelium (RPE) present additional hurdles for delivery if the target location is the retinal tissues (Kim et al., 2007). Drug delivery is even more challenging for macromolecules such as proteins because permeability through the sclera decreases exponentially with the molecular radius (Edwards and Prausnitz, 1998; Ambati et al., 2000). To overcome these transport barriers, the intrascleral flux must be increased. In this report, we describe a novel and non-invasive approach employing ultrasound to enhance the intrascleral delivery of proteins.

The application of short duration (30 s), medium-frequency (1 MHz) ultrasound (Merino et al., 2003; Benwell and Bly, 1987) at low power (0.05 W/cm^2) imposes physical modulation to the barrier property of the rabbit sclera, as reflected by a significant increase in the depth of penetration by FITC–BSA (Fig. 2). We used FITC–BSA, a 65 kDa protein measuring 3.62 nm in hydrodynamic radius, as a model macromolecular drug. Experiments were performed to understand the characteristics and nature of ultrasound-mediated intrascleral delivery. We investigated the role of the bulk flow due to acoustic streaming. Acoustic streaming is the movement of fluid due to the energy transfer from the ultrasound wave to the fluid. The flow current is unidirectional, along the ultrasound beam and away from the transducer (Clarke et al., 2004; Lavon and Kost, 2004). We have ruled out this ultrasound-induced bulk flow as the major mechanism since penetration immediately after ultrasound treatment is limited (Fig. 5). Instead, enhanced diffusion is observed after ultrasound application (Figs. 2 and 7). The observation that the penetration distance is proportional to the square root of time indicates that FITC–BSA is transported into the sclera by diffusion (Saltzman, 2001).

Next, we ask whether the thermal or non-thermal effect is the main contributor. Due to the low energy input, the temperature rise was less than 0.5 °C on the scleral surface. According to the Stokes–Einstein equation, diffusivity increases proportionally with absolute temperature. Thus this minor temperature increase cannot account for the increase in diffusivity (Fig. 7 and Supplementary information).

The non-thermal effects of ultrasound include mechanical stress and cavitation. Mechanical stress is due to the induction of sinusoidal pressure variations in a medium by the longitudinal wave of ultrasound. This wave would cause density variations on a medium, causing cyclic stress on a material and leading to fatigue. This phenomenon has been reported in polymers and metals and the effect is proportional to the ultrasound frequency (Van Krevelen, 1976). However, mechanical stress on the sclera cannot be used to explain the improvement in protein transport. When we increased the ultrasound frequency to 3 MHz, the penetration distance dropped compared to the 1 MHz experiment, and was at a value similar to the untreated eye (Fig. 6). This result points to the contribution of cavitation as the likely explanation, since the effect of cavitation is known to decrease with ultrasound frequency (Lavon and Kost, 2004).

Cavitation is the formation of bubbles and their subsequent dynamics (Atchley and Crum, 1988). Ultrasound-induced cavitation is used to enhance transdermal drug delivery (Merino et al., 2003) and accelerate fibrinolysis (Blinc et al., 1993). The large-scale variations in the bubble's size (relative to the equilibrium size) over a few acoustic cycles causing a violent collapse of bubbles and the subsequent release of energy, a phenomenon termed transient (or inertial) cavitation, is used to explain the augmented delivery of large and hydrophilic molecules through the skin by low-frequency ultrasound. The shock waves and/or microjets created by cavitation disrupt the lipid bilayer in the stratum corneum and generate aqueous transport pathways (Merino et al., 2003). In fibrinolysis, medium-frequency ultrasound is used to improve the transport of proteins including plasminogen into the blood clot. The enhancement is attributed to stable (or non-inertial) cavitation, which involves small-scale oscillations of bubbles about an equilibrium radius (Atchley and Crum, 1988). Furthermore, microstreaming due to a stable cavitation has been proposed as the mechanism that reversibly changes the fiber structure in a fibrin gel, resulting in a drop of the resistance against protein transport (Collis et al., 2010; Braaten et al., 1997; Perren et al., 2008). Microstreaming is small-scale streaming or circulation which can occur at the oscillatory boundary surrounding a pulsating bubble driven by the sound field. High and localized shear stress is produced due to the large velocity gradient over a short length scale (Coussios and Roy, 2008; Leighton, 1994b).

At present, our data suggest that the enhancement in intrascleral protein delivery is related to stable cavitation. We have confirmed the presence of bubble activity from stable cavitation by detecting peaks at harmonic frequencies on the frequency spectrum (Fig. 7a). According to the theoretical prediction for stable cavitation, the lowest threshold for ultrasound wave of 1–4 MHz to generate rectified diffusion and acoustic streaming corresponds to an intensity range from 0.003 to 0.03 W/cm^2 (Lewin and Bjorno, 1982). Thus, The ultrasound parameters we used in the experiments (1 MHz, 0.05 W/cm^2, continuous wave) produced sufficient acoustic pressure to generate oscillating bubbles at the resonant size (with radius about 3 μm (Leighton, 1994a)) and induce microstreaming. On the other hand, we did not detect subharmonic peaks corresponding to transient cavitation on the frequency spectrum (Fig. 7b). The absence of transient cavitation was also supported by theoretical estimation (Holland and Apfel, 1989). Based on the theory, we found that the minimum intensity to achieve transient cavitation is 1.4 W/cm^2 at 1 MHz (Supplementary information), much higher than the intensity used in our experiments. However, our results did not reveal the relative importance between stable and transient cavitation in enhancing intrascleral delivery. Further investigation about the detailed mechanism of ultrasound-mediated enhancement is warranted.

The structure of sclera, though different from stratum corneum and fibrin clot, is amenable for disturbance by ultrasound. Sclera has only a sparse population of fibroblasts. The connective tissue is mainly a mesh composed of interlacing fiber bundles rich in collagen and elastin, surrounded by randomly oriented proteoglycan fibers (Hay, 1981; Watson and Young, 2004). The effective diffusivity of macromolecules through this fibrous structure is directly proportional to porosity and inversely proportional to tortuosity (Saltzman, 2001). It is possible that cavitation loosens the elastic fiber network and creates more open channels for protein transport. Ultrasound energy may also non-covalently modify the proteoglycan fiber morphology, similar to its effect on fibrin fibers and self-assembled peptide fibers (Braaten et al., 1997; Yokoi et al., 2005). Edwards and Prausnitz applied the fiber matrix theory to mathematically model the solute permeability through the sclera and predicted that a change in the proteoglycan architecture could reduce the diffusional resistance against macromolecules (Edwards and Prausnitz, 1998).

The acellular and fibrous nature of the sclera also helps to explain why it is capable of restoring the barrier function shortly after ultrasound treatment and why the ultrasound enhancement is repeatable. We found a temporary window of about 15 min in which the protein penetration was enhanced (Figs. 2 and 3). Consistent with the observation that ultrasound effect was temporary, the intrascleral diffusivity was increased in the first 15 min but decreased to a value comparable to the control afterwards (Fig. 7). When ultrasound was re-applied, similar augmentation of protein penetration was found (Fig. 4). This observation is consistent with our argument that the transport is enhanced by the ultrasound's physical disturbance of the fiber structures and not a permanent damage to living cells. Un-stretching of elastic fibers and resuming of the original pore structure are probable upon the termination of ultrasound application. Re-assembly of disaggregated fibers, driven by thermodynamics, will take place after ultrasound treatment ends. Another cycle of fiber restructuring is initiated when ultrasound is reapplied, allowing repeated delivery. After therapeutic molecules are delivered, it is important for the scleral barrier to reseal for eye protection. The data demonstrated that ultrasound application using the current settings caused no permanent change to the sclera's resistance against macromolecular transport.

Using the current settings, the increase in diffusivity by ultrasound is statistically significant. However, the magnitude is modest (1.6-folds). This level of enhancement may increase the drug concentration inside the sclera, and benefit the treatment of diseases at the uvea (e.g. uveitis). However, it should also be pointed out that sclera may not be the only barrier for transscleral protein delivery, the conjunctiva and dynamic clearance may present other barriers for protein delivery *in vivo*. The importance of these proof-of-concept experiments is that they demonstrate feasibility and shed light on the underlying mechanism, thus showing directions for optimization. When transscleral flux is further increased, it is possible to overcome the dynamic clearance from the choroidal circulation and augment the diffusive drive across the retinal pigmented epithelium, benefiting disease treatment at the choroid and retina. The lowest frequency (1 MHz) used in this study was within the medium range. Since cavitation is now deduced to be the dominant mechanism, and it is known that the efficiency of cavitation is inversely proportional to ultrasound frequency (Lavon and Kost, 2004), we hypothesize that the intrascleral flux of protein can be further increased by decreasing the ultrasound frequency to the low frequency regime (20–100 kHz). Experiments are now underway to investigate the frequency dependence.

We have intentionally selected to operate at a low energy level to limit the temperature rise due to the safety concern caused by heating ocular tissues (Rockville, 1997). For diagnostic applications using ultrasound, the regulatory requirement allows a maximum increase of 1 °C and the observed temperature rise was well below this cutoff even in the absence of blood circulation. In addition, FDA recommends a mechanical index (which gives a measure of the non-thermal damage by ultrasound) below 0.23. The estimated value from the current settings was well below this limit (Supplementary information). To verify that ultrasound application did not compromise the structure of the retinal tissues, they were examined histologically (Fig. 8). The morphological appearance of the eye especially of the retinal layer which was indirectly involved did not show any apparent abnormality as compared to the normal untreated control. The low intensity ultrasound exposure did not cause any adverse effect of the retina or its detachment.

Instead of using a diffusion chamber, we opted for an *ex vivo* set up that preserved the entire eyeball during ultrasound treatment. This method ensures the intactness of the ocular tissues and maintains the intraocular pressure. We notice that the passive intrascleral diffusivity measured using this set up is similar to the data reported by Maurice and Polgar (1977), but lower than some other reports in literature (Ambati et al., 2000; Cruysberg et al., 2005; Anderson et al., 2008). The difference may be due to the variation in the setup by different groups.

5. Conclusion

This report shows for the first time that it is feasible to use ultrasound to enhance protein delivery into the sclera. Equally important is the conclusion that the weakening of the scleral barrier is not permanent nor is there any observable damage to the retinal tissue. This approach should, in addition to microneedles and iontophoresis, provide a non-invasive alternative to deliver drugs inside the sclera, placing them closer to the Bruch's membrane-choroid where neovascularization occurs in sight-threatening diseases (e.g. wet age-related macular degeneration). *In vivo* studies will be required to firmly establish the usefulness of ultrasound-enhanced delivery of protein in practical applications.

Acknowledgements

The authors thank The Hong Kong Research Grant Council (RPC06/07.EG11) and the Innovation and Technology Fund (ITS/174/09) for financial support.

Appendix A. Supplementary data

Supplementary data associated with this article can be found, in the online version, at doi:10.1016/j.ijpharm.2010.09.001.

References

Ambati, J., Canakis, C.S., Miller, J.W., Gragoudas, E.S., Edwards, A., Weissgold, D.J., Kim, I., Delori, F.C., Adamis, A.P., 2000. Diffusion of high molecular weight compounds through sclera. Invest. Ophthalmol. Vis. Sci. 41, 1181–1185.

Anderson, O.A., Jackson, T.L., Singh, J.K., Hussain, A.A., Marshall, J., 2008. Human transscleral albumin permeability and the effect of topographical location and donor age. Invest. Ophthalmol. Vis. Sci. 49, 4041–4045.

Atchley, A.A., Crum, L.A., 1988. Acoustic cavitation and bubble dynamics. In: Suslick, K.S. (Ed.), Ultrasound: Its Chemical, Physical, and Biological Effects. VCH Publishers, New York.

Benwell, A.D., Bly, S.H.P., 1987. Sources and applications of ultrasound. In: Repacholi, M., Grandolfo, M., Rindi, A. (Eds.), Ultrasound: Medical Application, Biological Effects and Hazard Potentials. Plenum Press, New York, pp. 29–47.

Blinc, A., Francis, C.W., Trudnowski, J.L., Carstensen, E.L., 1993. Characterization of ultrasound-potentiated fibrinolysis in vitro. Blood 81, 2636–2643.

Braaten, J.V., Goss, R.A., Francis, C.W., 1997. Ultrasound reversibly disaggregates fibrin fibers. J. Thromb. Haemost. 78, 1063–1068.

Clarke, L., Edwards, A., Graham, E., 2004. Acoustic streaming: an in vitro study. Ultrasound Med. Biol. 30, 559–562.

Collis, J., Manasseh, R., Liovic, P., Tho, P., Ooi, A., Petkovic-Duran, K., Zhu, Y., 2010. Cavitation microstreaming and stress fields created by microbubbles. Ultrasonics 50, 273–279.

Coussios, C.C., Roy, R.A., 2008. Applications of acoustics and cavitation to noninvasive therapy and drug delivery. Annu. Rev. Fluid Mech. 40, 395–420.

Cruysberg, L.P.J., Nuijts, R.M.M.A., Geroski, D.H., Gilbert, J.A., Hendrikse, F., Edelhauser, H.F., 2005. The influence of intraocular pressure on the transscleral diffusion of high-molecular-weight compounds. Invest. Ophthalmol. Vis. Sci. 46, 3790–3794.

Edward, J.T., 1970. Molecular volumes and the Stokes–Einstein equation. J. Chem. Educ. 47, 261–270.

Farny, C.H., Holt, R.G., Roy, R.A., 2009. Temporal and spatial detection of Hifu-induced inertial and hot-vapor cavitation with a diagnostic ultrasound system. Ultrasound Med. Biol. 35, 603–615.

Edwards, A., Prausnitz, M.R., 1998. Fiber matrix model of sclera and corneal stroma for drug delivery to the eye. AIChE J. 44, 214–225.

Geroski, D.H., Edelhauser, H.F., 2001. Transscleral drug delivery for posterior segment disease. Adv. Drug Deliv. Rev. 52, 37–48.

Hamalainen, K.M., Kananen, K., Auriola, S., Kontturi, K., Urtti, A., 1997. Characterization of paracellular and aqueous penetration routes in cornea, conjunctiva, and sclera. Invest. Ophthalmol. Vis. Sci. 38, 627–634.

Hay, E.D., 1981. Cell Biology of Extracellular Matrix. Plenum Press, New York.

Janoria, K.G., Gunda, S., Boddu, S.H., Mitra, A.K., 2007. Novel approaches to retinal drug delivery. Expert Opin. Drug Deliv. 4, 371–388.

Holland, C.K., Apfel, R.E., 1989. An improved theory for the prediction of microcavitation thresholds. IEEE Trans. Ultrason. Ferroelectr. Freq. Control. 36, 204–208.

Jiang, J., Moore, J.S., Edelhauser, H.F., Prausnitz, M.R., 2009. Intrascleral drug delivery to the eye using hollow microneedles. Pharm. Res. 26, 395–403.

Kim, S.H., Lutz, R.J., Wang, N.S., Robinson, M.R., 2007. Transport barriers in transscleral drug delivery for retinal diseases. Ophthal. Res. 39, 244–254.

Kourlas, H., Abrams, P., 2007. Ranibizumab for the treatment of neovascular age-related macular degeneration: a review. Clin. Ther. 29, 1850–1861.

Kremer, F.B., Walton, P., Gensheimer, G., 1985. Determination of corneal thickness using ultrasonic pachometry. Ann. Ophthalmol. 17, 506–507.

Leighton, T.G., 1994a. The Acoustic Bubble. Academic Press, London.

Leighton, T.G., 1994b. Acoustic bubble detection. I. The detection of stable gas bodies. Environ. Eng. 7, 9–16.

Leighton, T.G., 1995. Acoustic bubble detection. II. The detection of transient cavitation. Environ. Eng. 8, 16–25.

Lavon, I., Kost, J., 2004. Ultrasound and transdermal drug delivery. Drug Discov. Today 9, 670–676.

Lewin, P.A., Bjorno, L., 1982. Thresholds for rectified diffusion and acoustic microstreaming by bubbles in biological tissue. Appl. Sci. Res. 38, 25–35.

Maurice, D.M., Polgar, J., 1977. Diffusion across sclera. Exp. Eye Res. 25, 577–582.

McDermott, M.L., Puklin, J.E., Abrams, G.W., Eliott, D., 1997. Phacoemulsification for cataract following pars plana vitrectomy. Ophthal. Surg. Lasers 28, 558–564.

Merino, G., Kalia, Y.N., Guy, R.H., 2003. Ultrasound-enhanced transdermal transport. J. Pharm. Sci. 92, 1125–1137.

Mitragotri, S., Blankschtein, D., Langer, R., 1995. Ultrasound-mediated transdermal protein delivery. Science 269, 850–853.

Myles, M.E., Neumann, D.M., Hill, J.M., 2005. Recent progress in ocular drug delivery for posterior segment disease: emphasis on transscleral iontophoresis. Adv. Drug Deliv. Rev. 57, 2063–2079.

Nomoto, H., Shiraga, F., Kuno, N., Kimura, E., Fujii, S., Shinomiya, K., Nugent, A.K., Hirooka, K., Baba, T., 2009. Pharmacokinetics of bevacizumab after topical, subconjunctival, and intravitreal administration in rabbits. Invest. Ophthalmol. Vis. Sci. 50, 4807–4813.

Parkinson, T.M., Ferguson, E., Febbraro, S., Bakhtyari, A., King, M., Mundasad, M., 2003. Tolerance of ocular iontophoresis in healthy volunteers. J. Ocul. Pharmacol. Ther. 19, 145–151.

Pavlin, C.J., Harasiewicz, K., Sherar, M.D., Foster, F.S., 1991. Clinical use of ultrasound biomicroscopy. Ophthalmology 98, 287–295.

Perren, F., Loulidi, J., Poglia, D., Landis, T., Sztajzel, R., 2008. Microbubble potentiated transcranial duplex ultrasound enhances IV thrombolysis in acute stroke. J. Thromb. Thrombol. 25, 219–223.

Prince, J.H., McConnell, D.G., 1964. The Rabbit in the Eye Research. Charles C Thomas, Springfield, IL.

Rockville, M., 1997. In: Administration, F.D.A. (Ed.), Information for Manufacturers Seeking Marking Clearance of Diagnostic Ultrasound Systems and Transducers. Center for Devices and Radiological Health.

Saltzman, W.M., 2001. Drug Delivery—Engineering Principles for Drug Therapy. Oxford University Press, Inc., New York.

Sieving, P.A., Caruso, R.C., Tao, W., Coleman, H.R., Thompson, D.J., Fullmer, K.R., Bush, R.A., 2006. Ciliary neurotrophic factor (CNTF) for human retinal degeneration: phase I trial of CNTF delivered by encapsulated cell intraocular implants. Proc. Natl. Acad. Sci. U. S. A. 103 (10), 3896–3901.

Van Krevelen, D.W., 1976. Properties of Polymers, Their Estimation and Correction with Chemical Structure. Elsevier, New York.

Watson, P.G., Young, R.D., 2004. Scleral structure, organisation and disease. A review. Exp. Eye Res. 78, 609–623.

Yokoi, H., Kinoshita, T., Zhang, S., 2005. Dynamic reassembly of peptide RADA16 nanofiber scaffold. Proc. Natl. Acad. Sci. U. S. A. 102, 8414–8419.

Zarbin, M., Szirth, B., 2007. Current treatment of age-related macular degeneration. Optom. Vis. Sci. 84, 559–572.

Zderic, V., Clark, J.I., Martin, R.W., Vaezy, S., 2004a. Ultrasound-enhanced transcorneal drug delivery. Cornea 23, 804–811.

Zderic, V., Clark, J.I., Vaezy, S., 2004b. Drug delivery into the eye with the use of ultrasound. J. Ultrasound Med. 23, 1349–1359.

Zderic, V., Vaezy, S., Martin, R.W., Clark, J.I., 2002. Ocular drug delivery using 20-kHz ultrasound. Ultrasound Med. Biol. 28, 823–829.